

Doppler-free high resolution continuous wave optical UV-spectroscopy on the $A^2\Sigma^+ \leftarrow X^2\Pi_{3/2}$ transition in nitric oxide

Patrick Kaspar¹, Fabian Munkes¹, Philipp Neufeld¹, Lea Ebel¹, Yannick Schellander², Robert Löw¹, Tilman Pfau¹, and Harald Kübler¹

¹ University of Stuttgart, 5. Institute of Physics and Center for Integrated Quantum Science and Technology IQST, Pfaffenwaldring 57, 70569 Stuttgart, Germany

² University of Stuttgart, Institute for Large Area Microelectronics, Allmandring 3b, 70569 Stuttgart, Germany

E-mail: h.kuebler@physik.uni-stuttgart.de

June 2022

Abstract. We report on Doppler-free continuous-wave optical UV-spectroscopy resolving the hyperfine structure of the $A^2\Sigma^+ \leftarrow X^2\Pi_{3/2}$ transition in nitric oxide for total angular momenta $J_X = 1.5 - 19.5$ on the oP_{12ee} branch. The resulting line splittings are compared to calculated splittings and fitted determining new values for the molecular constants b , c , eQq_0 and b_F for the $A^2\Sigma^+$ state. The constants are in good agreement with values previously determined by quantum beat spectroscopy.

1. Introduction

Nitric oxide (NO) has been subject to a large number of spectroscopic studies. It is of great interest to radio astronomy and atmospheric science [1, 2]. Especially the γ -band comprising the transitions between the two electronic states $A^2\Sigma^+$ and $X^2\Pi$ has been thoroughly investigated experimentally [3–9] and theoretically [10–12]. NO shows a hyperfine structure which is, for the most abundant isotope ($> 99\%$) $^{14}\text{N}^{16}\text{O}$, due to the nuclear spin $I = 1$ of nitrogen. The doublet ground state $X^2\Pi$ shows large spin-orbit splitting and Λ -type doubling. The latter was subject to the studies of Neumann [13] and Paul [14].

For the energetically lowered spin-orbit component $\Pi_{1/2}$ the Λ -type doubling is larger and increases linearly with J_X while the splitting in the $\Pi_{3/2}$ component is smaller but increases proportional to J_X^2 .

The hyperfine structure of the ground state has been investigated with different spectroscopic techniques. Early investigations relied on microwave spectroscopy [15–18]. Meerts and Dymanus [19] resolved several hyperfine transitions for both ground state manifolds for different total angular momenta J_X and provided matrix elements to treat the hyperfine structure with perturbation theory up to the third order. Further theoretical work was provided by Mizushima [20] and Kristiansen [21]. High precision infrared spectroscopy allowed the determination of hyperfine constants for the two spin-orbit components at the 10 Hz-level accuracy [22, 23].

In the excited state $A^2\Sigma^+$ spin-rotational splitting occurs [24, 25]. The hyperfine structure of the excited state was theoretically treated by Green [26, 27] and Walch [28]. First experimental results were published by Bergemann and Zare employing radio-frequency double resonance [29]. The $v = 1$ vibrational level was resolved via two-photon spectroscopy yielding fine and hyperfine parameters [30, 31]. In addition the electric dipole moment of the $A^2\Sigma^+$ state was investigated experimentally [32] and theoretically [33]. Reid observed hyperfine quantum beats with time-resolved photoelectron spectroscopy [34] while further measurements relied on two-color resonant four-wave mixing [35] and on quantum beat spectroscopy [36, 37].

Nitric oxide is involved in a multitude of chemical and biological processes in the human body [38–41]. It acts as an indicator for inflammatory diseases like asthma or cancer [42–44]. Therefore, detecting small amounts of nitric oxide in a large background of other gases is of particular interest in medical research. A novel approach to detect nitric oxide relies on optogalvanic detection. An optical excitation to Rydberg states is followed by collisional ionization and electrical detection of the thereby generated charges [45]. The working principle of this type of

sensing scheme has already been demonstrated in an idealized system and a proof of concept study [46, 47]. Employing narrow-band lasers instead of pulsed systems for the excitation increases the selectivity of such a sensor.

Within the scope of the development of a laboratory prototype sensor relying on narrow-band lasers, Doppler-free saturation spectroscopy was performed to gain precise knowledge of the substructure of the involved states. The resolved individual Lamb-Dips, which were also recently observed for the HD molecule [48, 49], are essential to quantify and assess the capabilities of the sensor prototype.

Doppler-free continuous wave spectroscopy was performed on the $\text{oP}_{12\text{ee}}$ branch of the $A^2\Sigma^+, (v=0) \leftarrow X^2\Pi_{3/2}, (v=0)$ transition for total angular momenta $J_X = 1.5$ to 19.5. The hyperfine structure has been partially resolved and corresponding hyperfine constants of the $A^2\Sigma^+$ state are fitted and compared to previously determined values. For the fit only data for $J_X > 5.5$ is included.

2. Experimental Methods

We employ Doppler-free saturated absorption spectroscopy [50] as depicted in figure 1. The laser source of the experiment is a frequency quadrupled titanium-sapphire laser tunable over the frequency range of the $A^2\Sigma^+, (v=0) \leftarrow X^2\Pi_{3/2}, (v=0)$ transition at 226 nm.

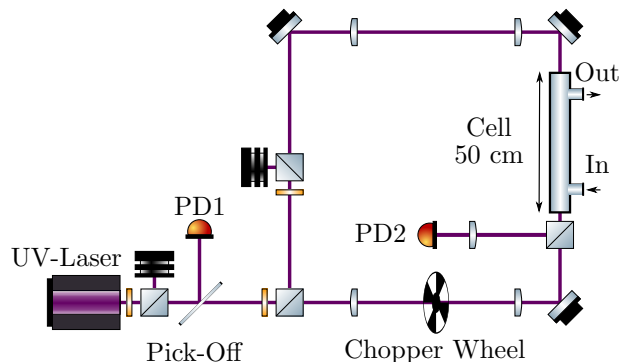


Figure 1. Schematic of the spectroscopy setup. The output of the UV-Laser is split into a pump and a probe beam which are both expanded before entering the cell in counter-propagating configuration. The pump beam is modulated with a chopper wheel to employ a lock-in amplifier.

The output power of the employed laser system is actively stabilized via a motorized halfwave-plate keeping the power on photodiode PD1 constant. The laser beam is split into a pump and a probe beam. These two beams enter the 50 cm long through flow spectroscopy cell in counter-propagating configuration with crossed linear polarizations. The probe beam is

detected on photodiode PD2 (Thorlabs PDA25K2 - GaP Switchable Gain Amplified Detector).

The laser power was set to 4 mW for the pump beam and 0.4 mW for the probe beam. Both beams are expanded, the pump beam to approximately 3.5 mm and the probe beam to 2.8 mm, to ensure that transient time broadening can be neglected. The beam diameters of the collimated beams were measured direct in front of the cell entrance. The slightly larger pump beam ensures a homogeneous illumination for the probe beam.

The lamb-dip signal is not visible without employing a lock-in amplifier to increase the signal to noise ratio. Therefore, the amplitude of the pump beam is modulated at a frequency of 9.8 kHz. An additional limitation is the frequency jitter of the UV-Laser occurring when the laser is scanned. This would lead to blurring and broadening of spectra which are averaged over several laser scans. To avoid this jitter the fundamental infrared beam of the quadrupled laser has to be stabilized. We employ an ultra-low expansion cavity to stabilize a master laser using the Pound-Drever-Hall technique [51]. The laser is sent on a transfer cavity and its length is stabilized to the master laser with the same technique using a piezo. The fundamental beam of the quadrupled Ti:Sa can then be sent on the transfer cavity. To stabilize the fundamental RF sidebands at two different frequencies are added using an electro-optic modulator (EOM). The sidebands needed to generate the Pound-Drever-Hall lock error signal are at a fixed frequency of 15 MHz. To be able to lock the laser at any desired frequency the second sideband frequency is tunable from $\Delta\omega/2\pi = 50$ MHz to $\Delta\omega/2\pi = 500$ MHz. The fixed sidebands and lock-sidebands are generated with different RF generators and added together by a power combiner. The lock-sidebands therefore also receive the fixed 15 MHz sidebands, so that it is possible to lock the laser to them.

Since nitric oxide dissociates rapidly under UV radiation [52, 53] it is not possible to acquire comparable sets of data with a sealed spectroscopy cell. Therefore, the employed cell is connected to a vacuum pump system comprising a membrane and turbo pump to realize a controlled through flow system. Between the outlet of the cell and the turbo pump, a choke system is installed limiting the suction power of the turbo pump by adjusting two butterfly valves. First the pressure is coarsely adjusted with the choke system. A constant pressure and flow is then ensured by a mass flow controller (MFC) in front of the cell. It is set so, to obtain a minimal pressure difference between the two gauges monitoring the pressure. They are positioned directly at the inlet and outlet of the cell. Once the desired pressure is reached and the

system is in equilibrium it is stable without the need of further adjustments on the MFCs or choke. The flow is regulated to an accuracy of 0.2% to 1.0% depending on the set value. The mean pressure was set to be around 0.0230 mbar for all datasets presented.

The procedure to record a spectrum as shown in figure 2 is as follows. First a continuous flow of NO is set and the laser is tuned to the coarse frequency of the desired rotational transition by referring to a wavemeter. As a next step, the laser is scanned over a frequency range spanning several GHz to find the absorption profile of the corresponding spectral line. Since the experiment is conducted at room temperature, rotational lines are broadened by the Doppler-effect resulting in a linewidth of around 3 GHz. The laser scan width is then lowered stepwise to position the scan around the center of the absorption feature. For stronger rotational transitions the Lamb-dip is already visible without averaging the lock-in signal. This is beneficial for adjusting the beam overlap to achieve maximum signal strength while minimizing any reflection of the pump beam onto the detector PD2. The laser can now be locked to the approximate position of the Lamb-dip or if it is not visible to the center of the Doppler-broadened absorption line by tuning the frequency of the lock-sidebands accordingly. In any case, before the actual measurement a coarse EOM-scan is performed. Then the laser frequency is changed in steps of 2 MHz up to a detuning of -80 MHz. For each frequency step a full integration cycle of the lock-in amplifier is collected. For coarse scans the time constant of the lock-in amplifier is set to 1 s. If the lamb dip is visible on the coarse scan, a fine scan is performed. Otherwise the procedure is repeated for a different or larger frequency interval. For finer scans the frequency step size of the laser is set to 0.4 MHz and the time constant of the lock-in amplifier to 10 s.

3. Results

The measurements on the oP_{12ee} branch yield Lamb-dip spectra for the total angular momenta $J_X = 1.5$ to 19.5. The corresponding total angular momentum of the excited state is given by $J_A = J_X - 1$. A selection of the recorded spectra is shown in figure 2. Peak ③ was set to zero detuning so that all other frequencies are given relative. In the range $J_X = 6.5$ to 19.5 three individual hyperfine transitions (Lamb-dips) were resolved. With decreasing J_X the splitting between the transitions decreases. In figure 2h lines ① and ② have merged together so that only a single splitting can be determined. Therefore data for $J < 6.5$ was not used for further evaluation. At a later point, comparison of the data to a calculated spectrum

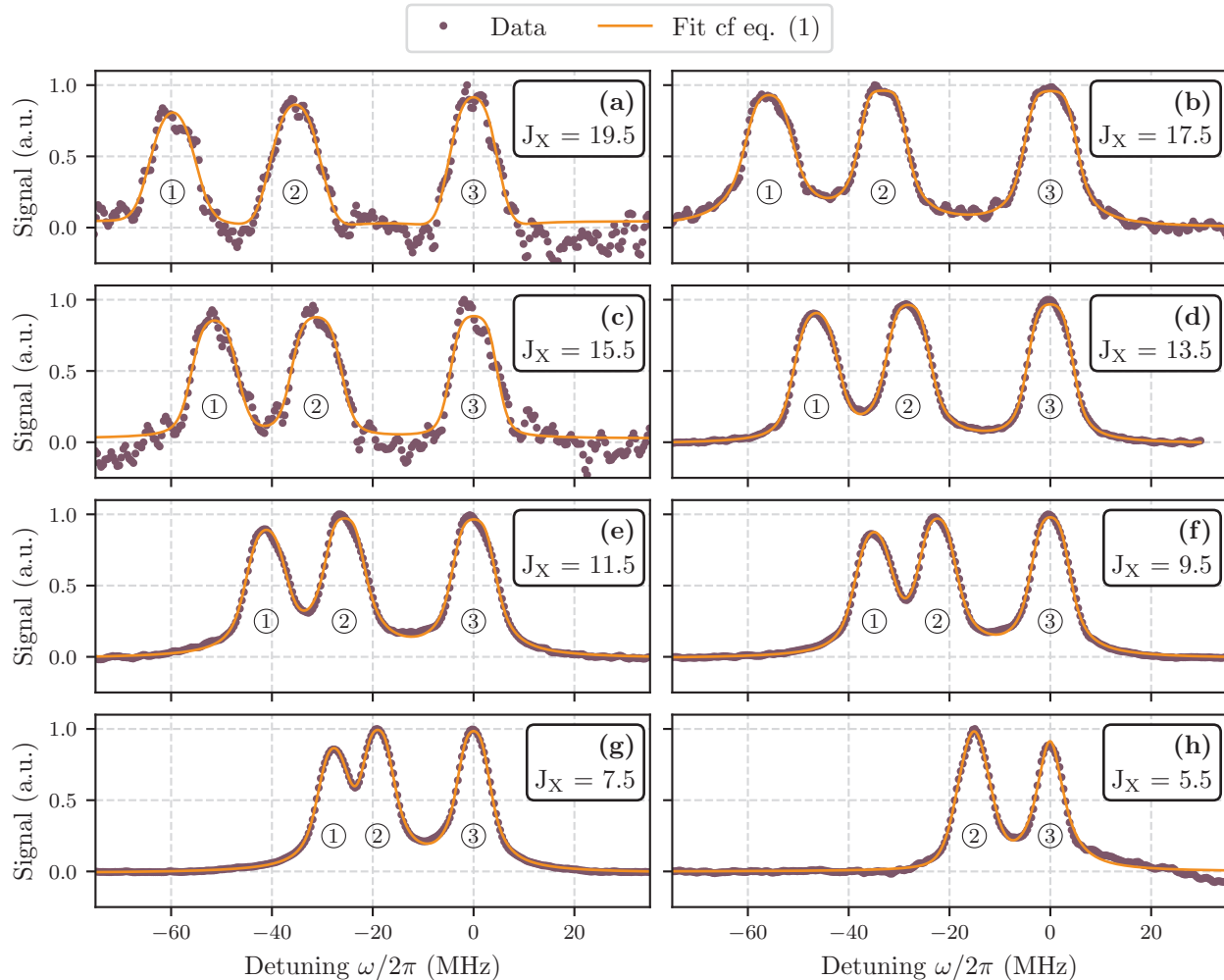


Figure 2. Selection of measured hyperfine spectra for different total angular momenta between (a) $J_X = 19.5$ and (h) 5.5 . The data is shown as violet dots and was fitted with a Voigt profile of the form given in equation 1, shown as orange lines.

will show that the decrease of the line splittings is the expected behavior, see figure 4.

Since the beam overlap changed in between individual measurements and the mode of the UV-Laser is not gaussian, the linewidth of the data will not be discussed. Our evaluation will focus on the splittings between the individually resolved lines instead. These are due to the energy structure of the molecule and not influenced by parameters like pressure, laser power or beam overlap. To determine the splitting between the measured hyperfine transitions the data was fitted with a Voigt-profile in a Lambert-Beer envelope after baseline and offset correction. The corresponding function is given in equation 1 and depicted in figure 2 as orange line,

$$V(z) = A \cdot \left(1 - \exp \left(-1 \cdot \sum_{k=1}^3 \operatorname{Re} [w_k(z(f))] \right) \right). \quad (1)$$

Here A is the overall amplitude and $w_k(z)$ the Fadeeva function

$$w_k(z) = \exp(-z^2) \left(1 + \frac{2i}{\sqrt{\pi}} \int_0^z \exp(t^2) dt \right). \quad (2)$$

The argument z of the normalized Fadeeva function is given by

$$z(f) = \frac{f - f_0 + i\gamma}{\sqrt{2}\sigma}. \quad (3)$$

It includes most of the remaining fit parameters, which are the frequency position of the maximum f_0 , the Lorentzian linewidth γ and the Doppler width σ of the Voigt profile. The sum takes into account the number of peaks in the spectrum and f is the measured frequency. From the fitparameter f_0 the splitting between the fitted lines can be calculated and compared to theoretically calculated values.

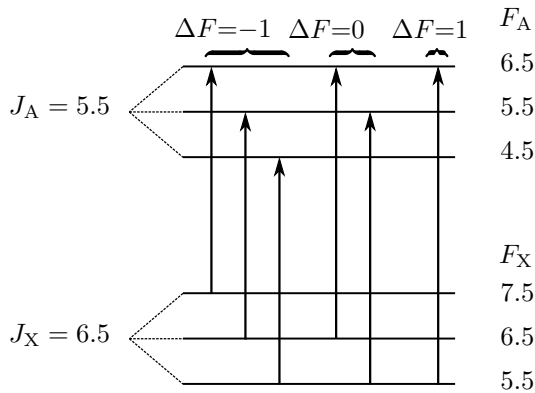


Figure 3. Schematic of the of the six expected hyperfine transitions for an exemplary rotational transition of the oP_{12ee} branch. The energy splittings and arrows are not to scale.

As already mentioned the hyperfine structure is only partially resolved. Figure 3 shows a schematic level scheme for all hyperfine transitions of a single rotational transition of the measured P-branch. According to the dipole selection rule for hyperfine transitions $\Delta F = \pm 1, 0$, one expects a total of six hyperfine transitions to show up: Three transitions with $\Delta F = -1$, two transitions with $\Delta F = 0$ and one with $\Delta F = +1$. To assign which of the six possible transitions were resolved, a full spectrum of the NO γ -band has been calculated using the software *pgopher* [54]. The calculation is based on the constants given in table 1.

It yields the six expected hyperfine transitions. However, there is a significant intensity difference between the transitions. The strongest three lines correspond to transitions with $\Delta F = -1$. They appear roughly 10 to 100 times stronger than the remaining two lines belonging to $\Delta F = 0$ transitions and the line belonging to the $\Delta F = +1$ transition is significantly weaker than the $\Delta F = 0$ lines. This is the case because for $\Delta F = -1$ transitions only the orbital angular momentum of the electron has to be changed. For the $\Delta F = 0, +1$ the nuclear spin has to change which leads to a smaller wavefunction overlap, thus a smaller transition dipole moment. Therefore we attribute the three measured transitions to $\Delta F = -1$ transitions. The calculated and measured splittings are depicted in figure 4(a). The violet and blue points represent measured data, the orange points correspond to the calculated splittings. The error bars include the fit error of the Voigt-fit and the estimated error of the laser stabilization which is the dominating contribution. It consists of the error of the master laser lock which is quadratically added to the error for the stabilization of the transfer cavity and the error of the lock of the laser itself. The total error due to the laser stabilization is around 450 kHz for the fundamental

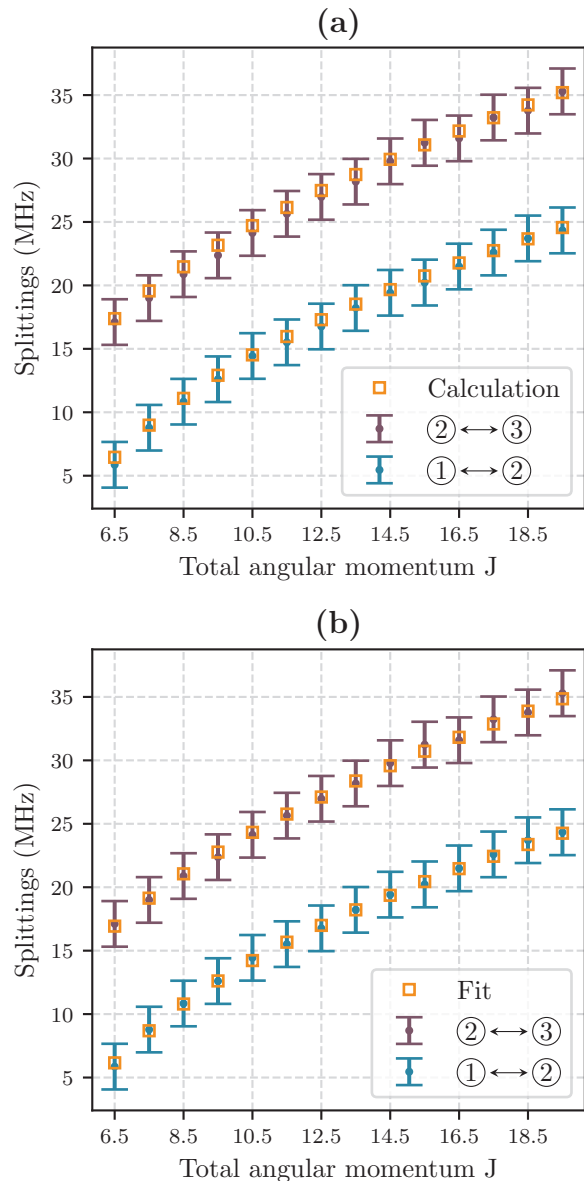


Figure 4. (a) Comparison between measured and calculated hyperfine splittings. The measured splittings were calculated from the fit parameters of the Voigt-fit shown in figure 2. The errorbars include the estimated error of the laser lock and one standard deviation of the fit error. (b) Experimentally measured splittings as shown in (a) compared to data calculated from the newly fitted hyperfine constants for the $A^2\Sigma^+$ state.

Table 1. List of constants used for the calculation with *pgopher*. All values are given in MHz.

$X^2\Pi$		
Constant	Value	Reference
B	50 848.130 72(18)	Varberg et al. [23]
D	0.164 141 19(31)	.
H	$3.774(15) \times 10^{-8}$.
A	3 691 813.855(12)	Varberg et al. [23]
A_D	5.372(38)	Danielak et al. [9]
γ	-193.987 9(77)	Varberg et al. [23]
γ_D	0.001 582 2(70)	.
p	350.405 443(91)	.
p_D	$3.78(18) \times 10^{-5}$.
q	2.822 100(51)	.
q_D	$4.370(38) \times 10^{-5}$.
q_H	$-8.6(25) \times 10^{-10}$.
a	84.203 78(76)	.
b_F	22.379 2(28)	.
b	42.006 5(38)	.
c	-58.882 0(32)	.
d	112.597 18(13)	.
d_D	$1.10(23) \times 10^{-4}$.
C_I	0.012347(52)	.
C'_I	0.007 37(36)	.
eQq_0	-1.856 71(26)	.
eQq_2	23.114 7(83)	Varberg et al. [23]
$A^2\Sigma^+$		
Constant	Value	Reference
$T_0^A - T_0^X$	1 323 308 163(60)	Danielak et al. [9]
B	59 545.297(293)	[9, 37]
D	0.169572(236)	[9, 37]
γ	-80.34(16)	[9, 37]
b_F	43.52(30)	Brouard et al. [37]
b	41.66(51)	.
c	5.59(64)	.
eQq_0	-7.31(23)	Brouard et al. [37]

laser, thus it then is 1.8 MHz in the UV. The lock errors were estimated via the root mean square of the noise of the error signal of the locked laser. In total the calculated and measured data show very good agreement.

In figure 4(b) the measured data is compared to data calculated from the newly fitted constants. The fitting was performed employing a wrapper program for the command line version of *pgopher* using a Levenberg-Marquardt algorithm for optimization. The hyperfine constants for the ground state of NO are very well determined [23] and were therefore kept fixed for the fitting procedure. The fine structure constants of the excited state were kept fixed as well. This leaves

Table 2. Fit results in MHz for the fitted hyperfine constants c, b, eQq_0 compared to the values from [37] used for the initial calculation (see figure 4(a) and to the closest previously determined value (CPV) with the corresponding source. An overview of the previously determined values for the respective constants is given in [37].

Constant	This work	Ref. [37]	CPV
c	5.29(53)	5.59(64)	5.59(64) [33]
b	41.06(9)	41.66(51)	41.66(51) [37]
eQq_0	-7.31(12)	-7.31(23)	-7.31(23) [37]
b_F	42.82(26)	43.52(30)	43.5(8) [32]

the three hyperfine constants c, b and eQq_0 of the $A^2\Sigma^+$ state to be fitted. From b and c the more convenient Fermi-contact constant b_F can be calculated $b_F = b + \frac{c}{3}$. The corresponding values of the molecular constants determined by the fit are listed in table 2 and compared to the values given in [37]. In addition the column CPV gives the previously determined value which is closest to the result of this work. The agreement between this work and [37] is particularly good for the quadrupole constant eQq_0 . In contrast, the dipole-dipole interaction of the nuclear spin with the electron spin c deviates from the previous value but is within the combined error bounds. The nuclear spin electron spin interaction constant b is just within the combined error bars. The Fermi-contact constant is in less good agreement with [37] as the other constants and lies closest to the value determined by [32]. Overall the constants determined in this work lie within the range of the previously determined values summarized in [37].

4. Summary

Doppler-free saturated absorption spectroscopy has been employed to investigate hyperfine transitions between the $X^2\Pi_{3/2}, v = 0$ ground state manifold and the $A^2\Sigma^+, v = 0$ state in nitric oxide. Spectra have been recorded for the oP_{12ee} branch with total angular momenta $J_X = 1.5 - 19.5$ of the ground state. The hyperfine structure resulting from the nuclear spin $I = 1$ in nitrogen has been partially resolved. The extracted hyperfine splittings in the range of $J_X = 5.5 - 19.5$ were discussed and compared to calculations based on previously determined constants which show good agreement with the data.

Furthermore the hyperfine constants b, c and eQq_0 for the $A^2\Sigma^+$ state were fitted. Comparison of the newly determined constants show good agreement with the constants measured by Brouard et al. [37]. Overall the new values presented in this work fit into the range of previously published theoretical and experimental

values.

For future experiments an even longer spectroscopy cell or a multipass-cell may be beneficial to measure at lower powers and pressures. This may increase the resolution further to resolve the weaker hyperfine lines. Measurement series for different laser powers and pressures may lead to a more precise determination of the yet only vaguely known saturation intensity and dynamical constants like excited state decay rates.

Decreasing the pressure by two orders of magnitude allowed narrower spectroscopic lines but only for rotational energy levels close to the maximum of the rotational energy distribution in the ground state. For other lines the signal to noise ratio was not sufficient for data analysis. Therefore a full, consistent set of data could not be obtained at those parameters, limiting the measurements to pressure broadened lines.

Acknowledgements

The authors thank the European Commission (Grant Agreement No. 820393, MACQSIMAL) for financial support. In addition the authors would like to thank Professor Edward Grant and Professor Stephen Hogan for fruitful discussions and valuable advice concerning the spectroscopic details of nitric oxide.

References

- [1] Altshuller A 1986 *Atmospheric Environment (1967)* **20** 245–268 ISSN 0004-6981 URL <https://www.sciencedirect.com/science/article/pii/0004698186900296>
- [2] Crutzen P J 1979 *Annual review of earth and planetary sciences* **7** 443–472
- [3] Hall R T and Dowling J M 1966 *The Journal of Chemical Physics* **45** 1899–1903 (Preprint <https://doi.org/10.1063/1.1727868>) URL <https://doi.org/10.1063/1.1727868>
- [4] Engleman R J, Rouse P E, Peek H M and Baiamonte V D 1969 URL <https://www.osti.gov/biblio/4128104>
- [5] Tajime T, Saheki T and Ito K 1978 *Appl. Opt.* **17** 1290–1294 URL <http://opg.optica.org/ao/abstract.cfm?URI=ao-17-8-1290>
- [6] Ishii J, Matsui T, Tsukiyama K and Uehara K 1994 *Chemical Physics Letters* **220** 29–34 ISSN 0009-2614 URL <https://www.sciencedirect.com/science/article/pii/0009261494001308>
- [7] Zobnin A V and Korotkov A N 1995 *Journal of Applied Spectroscopy* **61** URL <https://www.osti.gov/biblio/161866>
- [8] Wang D X, Haridass C and Reddy S 1996 *Journal of Molecular Spectroscopy* **175** 73–84 ISSN 0022-2852 URL <https://www.sciencedirect.com/science/article/pii/S0022285296900119>
- [9] Danielak J, Domin U, Ke R, Rytel M and Zachwieja M 1997 *Journal of Molecular Spectroscopy* **181** 394–402 ISSN 0022-2852 URL <https://www.sciencedirect.com/science/article/pii/S0022285296971817>
- [10] Langhoff S R, Bauschlicher C W and Partridge H 1988 *The Journal of Chemical Physics* **89** 4909–4917 (Preprint <https://doi.org/10.1063/1.455661>) URL <https://doi.org/10.1063/1.455661>
- [11] Cheng J, Zhang H and Cheng X 2017 *Computational and Theoretical Chemistry* **1114** 165–171 ISSN 2210-271X URL <https://www.sciencedirect.com/science/article/pii/S2210271X17302840>
- [12] Polák R and Fišer J 2003 *Chemical Physics Letters* **377** 564–570 ISSN 0009-2614 URL <https://www.sciencedirect.com/science/article/pii/S0009261403011795>
- [13] Neumann R 1970 *The Astrophysical Journal* **161** 779–784 URL <https://adsabs.harvard.edu/pdf/1970ApJ...161..779N>
- [14] Paul P 1997 *Journal of Quantitative Spectroscopy and Radiative Transfer* **57** 581–589 ISSN 0022-4073 URL <https://www.sciencedirect.com/science/article/pii/S0022407396001586>
- [15] Beringer R, Rawson E B and Henry A F 1954 *Phys. Rev.* **94**(2) 343–349 URL <https://link.aps.org/doi/10.1103/PhysRev.94.343>
- [16] Gallagher J J and Johnson C M 1956 *Phys. Rev.* **103**(6) 1727–1737 URL <https://link.aps.org/doi/10.1103/PhysRev.103.1727>
- [17] Favero P G, Mirri A M and Gordy W 1959 *Phys. Rev.* **114**(6) 1534–1537 URL <https://link.aps.org/doi/10.1103/PhysRev.114.1534>
- [18] Brown R L and Radford H E 1966 *Phys. Rev.* **147**(1) 6–12 URL <https://link.aps.org/doi/10.1103/PhysRev.147.6>
- [19] Meerts W and Dymanus A 1972 *Journal of Molecular Spectroscopy* **44** 320–346 ISSN 0022-2852 URL <https://www.sciencedirect.com/science/article/pii/002228527901099>
- [20] Mizushima M 1954 *Phys. Rev.* **94**(3) 569–574 URL <https://link.aps.org/doi/10.1103/PhysRev.94.569>
- [21] Kristiansen P 1977 *Journal of Molecular Spectroscopy* **66** 177–184 ISSN 0022-2852 URL <https://www.sciencedirect.com/science/article/pii/0022285277902077>
- [22] Saupe S, Meyer B, Wappelhorst M H, Urban W and Maki A G 1996 *Journal of Molecular Spectroscopy* **179** 13–21 ISSN 0022-2852 URL <https://www.sciencedirect.com/science/article/pii/S0022285296901794>
- [23] Varberg T D, Stroh F and Evenson K M 1999 *Journal of Molecular Spectroscopy* **196** 5–13 ISSN 0022-2852 URL <https://www.sciencedirect.com/science/article/pii/S0022285299978505>
- [24] Timmermann A and Wallenstein R 1981 *Optics Communications* **39** 239–242 ISSN 0030-4018 URL <https://www.sciencedirect.com/science/article/pii/0030401881901152>
- [25] Wallenstein R and Zacharias H 1978 *Optics Communications* **25** 363–367 ISSN 0030-4018 URL <https://www.sciencedirect.com/science/article/pii/0030401878901475>
- [26] Green S 1972 *Chemical Physics Letters* **13** 552–556 ISSN 0009-2614 URL <https://www.sciencedirect.com/science/article/pii/0009261472850097>
- [27] Green S 1973 *Chemical Physics Letters* **23** 115–119 ISSN 0009-2614 URL <https://www.sciencedirect.com/science/article/pii/0009261473895776>
- [28] Walch S P and Goddard W A 1975 *Chemical Physics Letters* **33** 18–24 ISSN 0009-2614 URL <https://www.sciencedirect.com/science/article/pii/0009261475854443>
- [29] Bergeman T and Zare R N 1974 *The Journal of Chemical Physics* **61** 4500–4514 (Preprint <https://doi.org/10.1063/1.1681767>) URL <https://doi.org/10.1063/1.1681767>
- [30] Murphy J, Bushaw B and Miller R 1993 *Journal of Molecular Spectroscopy* **159** 217–229 ISSN 0022-2852 URL <https://www.sciencedirect.com/science/article/pii/S0022285293001179>

- ticle/pii/S0022285283711197
- [31] Miller R J, Glab W L and Bushaw B A 1989 *The Journal of Chemical Physics* **91** 3277–3279 (Preprint <https://doi.org/10.1063/1.456903>) URL <https://doi.org/10.1063/1.456903>
- [32] Gray J A, Farrow R L, Durant J L and Thorne L R 1993 *The Journal of Chemical Physics* **99** 4327–4333 (Preprint <https://doi.org/10.1063/1.466086>) URL <https://doi.org/10.1063/1.466086>
- [33] Glendenning E D, Feller D, Peterson K A, McCullough E A and Miller R J 1995 *The Journal of Chemical Physics* **103** 3517–3525 (Preprint <https://doi.org/10.1063/1.470236>) URL <https://doi.org/10.1063/1.470236>
- [34] Reid K L, Duxon S P and Towrie M 1994 *Chemical Physics Letters* **228** 351–356 ISSN 0009-2614 URL <https://www.sciencedirect.com/science/article/pii/0009261494009635>
- [35] McCormack E F and Sarajlic E 2001 *Phys. Rev. A* **63**(2) 023406 URL <https://link.aps.org/doi/10.1103/PhysRevA.63.023406>
- [36] McCormack E, Pratt S, Dehmer P and Dehmer J 1994 *Chemical Physics Letters* **227** 656–662 ISSN 0009-2614 URL <https://www.sciencedirect.com/science/article/pii/0009261494008752>
- [37] Brouard M, Chadwick H, Chang Y P, Howard B J, Marinakis S, Screen N, Seamons S A and Via A L 2012 *Journal of Molecular Spectroscopy* **282** 42–49 ISSN 0022-2852 URL <https://www.sciencedirect.com/science/article/pii/S0022285212002172>
- [38] Furchgott R F and Zawadzki J V 1980 *Nature* **288** 373–376
- [39] Ignarro L, Buga G, Wood K, Byrns R and Chaudhuri G 1987 *Proc Natl Acad Sci USA* **84** 9265–9269
- [40] Yun H, Dawson V and Dawson T 1996 *Crit Rev Neurobiol* **10** 291–316 ISSN 0892-0915
- [41] Moncada S and Higgs E A 2006 *British Journal of Pharmacology* **147** S193–S201 ISSN 1476-5381 URL <https://dx.doi.org/10.1038/sj.bjp.0706458>
- [42] Alving K, Weitzberg E and Lundberg J 1993 *Eur Respir J* **6** 1368–1370
- [43] Lundberg J, Ehrén I, Jansson O, Adolfsson J, Lundberg J, Weitzberg E, Alving K and Wiklund N 1996 *Urology* **48** 700–702 ISSN 0090-4295 URL <https://www.sciencedirect.com/science/article/pii/S0090429596004232>
- [44] Mazzatenta A, Di Giulio C and Pokorski M 2013 *Respiratory Physiology & Neurobiology* **187** 128–134 ISSN 1569-9048 immunopathology of the Respiratory System URL <https://www.sciencedirect.com/science/article/pii/S1569904813000475>
- [45] Kaspar P, Munkes F, Schellander Y, Fabian J, Kasten M, Rubino L, Djekic D, Schalberger P, Baur H, Löw R, Pfau T, Anders J, Grant E, Frühauf N and Kübler H 2021 Towards an optogalvanic flux sensor for nitric oxide based on rydberg excitation *OSA Optical Sensors and Sensing Congress 2021 (AIS, FTS, HISE, SENSORS, ES)* (Optica Publishing Group) p STu4G.3 URL <http://opg.optica.org/abstract.cfm?URI=Sensors-2021-STu4G.3>
- [46] Schmidt J, Fiedler M, Albrecht R, Djekic D, Schalberger P, Baur H, Löw R, Frühauf N, Pfau T, Anders J, Grant E R and Kübler H 2018 *Applied Physics Letters* **113** 011113 (Preprint <https://doi.org/10.1063/1.5024321>) URL <https://doi.org/10.1063/1.5024321>
- [47] Schmidt J, Münzenmaier Y, Kaspar P, Schalberger P, Baur H, Löw R, Frühauf N, Pfau T and Kübler H 2020 *Journal of Physics B: Atomic, Molecular and Optical Physics* **53** 094001 URL <https://doi.org/10.1088/1361-6455/ab728e>
- [48] Tao L G, Liu A W, Pachucki K, Komasa J, Sun Y R, Wang J and Hu S M 2018 *Phys. Rev. Lett.* **120**(15) 153001 URL <https://link.aps.org/doi/10.1103/PhysRevLett.120.153001>
- [49] Diouf M L, Cozijn F M J, Darquié B, Salumbides E J and Ubachs W 2019 *Opt. Lett.* **44** 4733–4736 URL <http://opg.optica.org/ol/abstract.cfm?URI=ol-44-19-4733>
- [50] Foot C J 2005 *Atomic Physics* 1st ed (Great Clarendon Street, Oxford OX2 6DP: Oxford University Press) ISBN 0198506951
- [51] Drever R W P, Hall J L, Kowalski F V, Hough J, Ford G M, Munley A J and Ward H 1983 *Applied Physics B* **31**(2) 97–105 URL <https://doi.org/10.1007/BF00702605>
- [52] Minschwaner K and Starke V 2001 *Physics and Chemistry of the Earth, Part C: Solar, Terrestrial & Planetary Science* **26** 539–543 ISSN 1464-1917 URL <https://www.sciencedirect.com/science/article/pii/S1464191701000435>
- [53] Schellander Y 2020 *Ionization current measurements of Rydberg states in nitric oxide created by continuous-wave three-photon excitation* Master's thesis University of Stuttgart
- [54] Western C M 2017 *Journal of Quantitative Spectroscopy and Radiative Transfer* **186** 221–242 ISSN 0022-4073 satellite Remote Sensing and Spectroscopy: Joint ACE-Odin Meeting, October 2015 URL <https://www.sciencedirect.com/science/article/pii/S0022407316300437>